International Journal of Mathematics Trends and Technology Volume 68 Issue 8, 46-66, August 2022
ISSN: 2231-5373/ https://doi.org/10.14445/22315373/IJMTT-V68I8P506

Well Test Analysis of a Horizontal Well in a Completely Bounded Isotropic Reservoir

Bakary L. Marong [#1], Phineas Roy Kiogora [#2], Kennedy Otieno Awuor [*3]

[#1] Mathematics Department, Pan African University, Institute for Basic Sciences Technology and Innovation, Kenya

[*3] Mathematics and Acturial Science Department, Kenyatta University, Kenya

[#2] Mathematics Department, Jomo Kenyatta University of Agriculture and Technology, Kenya

Received: 30 June 2022 Revised: 01 August 2022 Accepted: 11 August 2022 Published: 24 August 2022

Abstract-A well test or well testing is consider as an elaborate plan of activity by an engineer to acquire, analyze and understand data about the properties of hydrocarbons which are trap below the surface of the earth in a reservoir and use the data to understand the reservoir itself. This study investigate the well test analysis of horizontal well in a completely bounded isotropic reservoir in a case where the non-dimensionalize flow parameters are plot on a log-log axis to analyze the pressure response in a horizontal well. It is also clear that horizontal well analysis is more difficult than vertical well analysis, because assessing the flow into a horizontal well requires three dimensions as oppose to a single flow for vertical wells. We develop five (5) well test analysis models to characterize a reservoir and predict the performance of a horizontal well, the non-dimensionalize flow parameters are plot on a log-log axis to analyze the pressure response in a horizontal well, we determine optimum well length for a horizontal well production. We use Source and Green's function with Newmann's product to develop the models, and we implement the results on matlab. We observe that from table 2 to table 11, as L_D increases both the P_D and $P_{D'}$ decreases when the well is initially open for production, this shows that dimensionless horizontal well length is inversely proportional to both the dimensionless pressure and dimensionless pressure derivative.

Keywords- early radial, dimensionless pressure, dimensionless pressure derivative, horizontal well, reservoir

I. INTRODUCTION

A well test or well testing can be considered as an elaborate plan of activities by an engineer to acquire, analyse and understand data about the properties of hydrocarbons which are trapped below the surface of the earth in a reservoir and also use the data to understand the reservoir itself. This data provides information about the ability of a reservoir to produce hydrocarbons.[1] observed that this whole process intents to obtain: reservoir pressure, completion efficiency, distance to the boundaries, formation damage, vertical layering, aerial extent, drawdown pressure, fluid properties, permeability, flow rates, formation heterogeneities, production capacity, productivity index, and other details relevant to the test. If this data can be obtained and analysed, well test analysis is the process where pressure transient analysis is conducted either to confirm production ability or to enhance performance.[13] noted that well test analysis to be considered as a wide area of reservoir engineering which involves the comprehension of the reservoir characteristics including the rock properties by applying different techniques.[2] noted that, this process provides information of both the well and the reservoir which contain the hydrocarbon in which well test analysis will involve the best model to interpret the pressure response. He noted that for an exploration well, the initial pressure, reservoir properties, nature and the rate of production would be the main objectives of a well test. For an appraisal well, one would need to conduct a well test to refine a reservoir description while for a development well, the well test would be used to adjust the reservoir description as well as establish pressure communication between wells.

The three main types of well testing methods that has been employed through several years are drawdown test, buildup test and Interference test.

In a drawdown test, a well which is shut-in is opened to flow. The main objectives of the drawdown test are to: obtain average permeability of the drainage area, estimate skin, obtain a pore of the reservoir and detect reservoir heterogeneity.

A producing well is shut down and a bottom hole pressure (BHP) is measured in a buildup test. To offer information on permeability and skin thickness for reservoir characterization. The results of a buildup test can also be used to monitor a reservoir, specifically reservoir pressure data.

Atleast two wells are employed in interference testing, the wells can be in the

same layer or different layer, and they can also be both horizontal or vertical wells or of different wells. The active well is put on production while the observational well is use to monitor the pressure and production rate and there is a pressure communication between the two wells in a reservoir. The observation well pressure response enables us to determine multiple well tests. We should observe when building an interference test, it will be preferable to build an active well rather than an injection well.

II. MATHEMATICAL DESCRIPTION

The governing equation of fluid flow in a horizontal oil reservoir is conforms to a non-linear, homogenous, isotropic, second order partial differential equation called the diffusivity equation. This equation is usually presented in 3D and is given by.

$$K_x \frac{\partial^2 P}{\partial x^2} + K_y \frac{\partial^2 P}{\partial y^2} + K_z \frac{\partial^2 P}{\partial z^2} = \phi \mu c_t \tag{1}$$

Since the reservoir is homogenous and isotropic, then $K_x = K_y = K_z$ where K_x, K_y and K_z are permeabilities along the x, y and z boundaries of the reservoir. ϕ is the porosity of the reservoir, μ is the reservoir fluid viscosity and c_t is total compressibility. Equation (1) is used to solve unsteady flow problems in porous media.

III. WELL TEST ANALYSIS MODELS

$$P_D = 2\pi h_D \int_0^{\tau_D} S(x_D, y_D, z_D, \tau_D) d\tau_D \tag{2}$$

(Gringarten and Ramey 1973)
where $t_D = \tau_D, dt_D = d\tau_D$

$$S(x_D, y_D, z_D, t_D) = S(x_D, t_D) \times S(y_D, t_D) \times S(z_D, t_D) \tag{3}$$

Equation (3) is the Newmann's product of the instantaneous source functions.

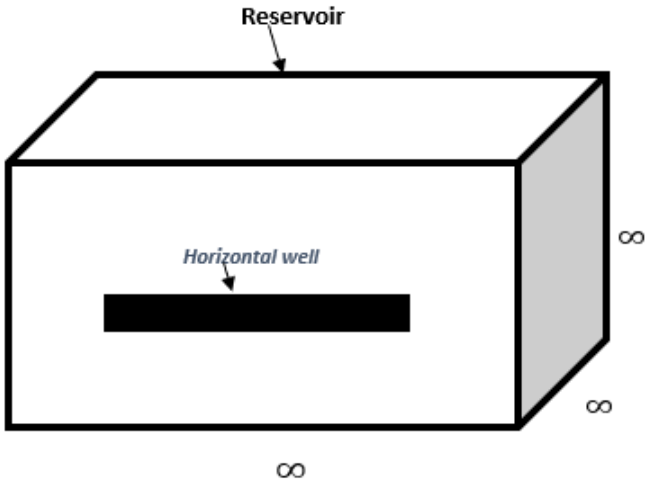

Figure 1:: 3D Reservoir physical model for Early Time Radial Flow

Early Time Approximation for Pressure

Considering a case where none of the boundaries is been affected by the flow, substituting the dimensionless variables in the greens and source function with Newman's product in equation (3) becomes.

$$S(x_D, \tau_D) = \frac{1}{2}[erf(\frac{\sqrt{\frac{K}{K_x}}+(x_D - x_{wD})}{2\sqrt{\tau_D}}) + erf(\frac{\sqrt{\frac{K}{K_x}}+(x_D - x_{wD})}{2\sqrt{\tau_D}})] \qquad (4)$$

Equation (4) is an Infinite-Acting flow along the x-boundary, which means x-boundary has not been affected by the flow. Therefore the pressure response is approximated within a short period of time.

$$S(y_D, \tau_D) = \frac{1}{2\sqrt{\pi\tau_D}}\sqrt{\frac{K}{K_y}}e^{-[\frac{(y_D - y_{wD})^2}{4_{\tau D}}]} \qquad (5)$$

Equation (5) is an Infinite-Acting flow along the y-boundary, which means y-boundary has not been affected by the flow. Therefore the pressure response is approximated within a short period of time.

For the Infinite-Acting flow, the flow along the y-boundary is the same as the flow along the z-boundary.

$$S(z_D,\tau_D)=\frac{1}{2\sqrt{\pi\tau_D}}\sqrt{\frac{K}{K_z}}[\exp(-\frac{(z_D-z_{wD})^2}{4\tau_D})] \quad (6)$$

Equation (6) is an Infinite-Acting flow along the z-boundary, which means z-boundary has not been affected by the flow. Therefore the pressure response is approximated within a short period of time.

Now by substituting equation (4), (5) and equation (6) into equation (2), we get.

$$P_D=2\pi h_D\int_0^{\tau_D}\{\frac{1}{2}[erf(\frac{\sqrt{\frac{K}{K_x}}+(x_D-x_{wD})}{2\sqrt{\tau_D}})+erf(\frac{\sqrt{\frac{K}{K_x}}+(x_D-x_{wD})}{2\sqrt{\tau_D}})]\}$$
$$\times\{\frac{1}{2\sqrt{\pi\tau_D}}\sqrt{\frac{K}{K_y}}e^{-[\frac{(y_D-y_{wD})^2}{4_{\tau D}}]}\}$$
$$\times\{\frac{1}{2\sqrt{\pi\tau_D}}\sqrt{\frac{K}{K_z}}[\exp(-\frac{(z_D-z_{wD})^2}{4\tau_D})]\}d\tau_D \quad (7)$$

The first part of equation (7) is the approximate form for instantaneous source function during early time in the x-boundary, the second part of equation is the approximate form for instantaneous function during early time in the y-boundary and the third part is the approximate form for instantaneous source function during early time in the z-boundary.

The dimensionless pressure derivatives for equation (7) is given by;

$$P_D'=2\pi h_D\{\frac{1}{2}[erf(\frac{\sqrt{\frac{K}{K_x}}+(x_D-x_{wD})}{2\sqrt{t_D}})+erf(\frac{\sqrt{\frac{K}{K_x}}+(x_D-x_{wD})}{2\sqrt{t_D}})]\}$$
$$\times\{\frac{1}{2\sqrt{\pi t_D}}\sqrt{\frac{K}{K_y}}e^{-[\frac{(y_D-y_{wD})^2}{4_{tD}}]}\}$$
$$\times\{\frac{1}{2\sqrt{\pi t_D}}\sqrt{\frac{K}{K_z}}[\exp(-\frac{(z_D-z_{wD})^2}{4t_D})]\} \quad (8)$$

This model presented by equation (7) and (8) applied in approximating pressure distribution for a horizontal well in a completely bounded oil reservoir for a short time when the flow is not being affected by any of the reservoir boundaries. This can be considered for a case once the well is initially put into production. Since none of the boundaries of the reservoir has any effect on the flow, the model thus considers a full infinite-acting flow period.

Effect of Boundaries on the Flow

Considering a case where x-boundary is not been affected by the flow, but y and z-boundaries are sealed.

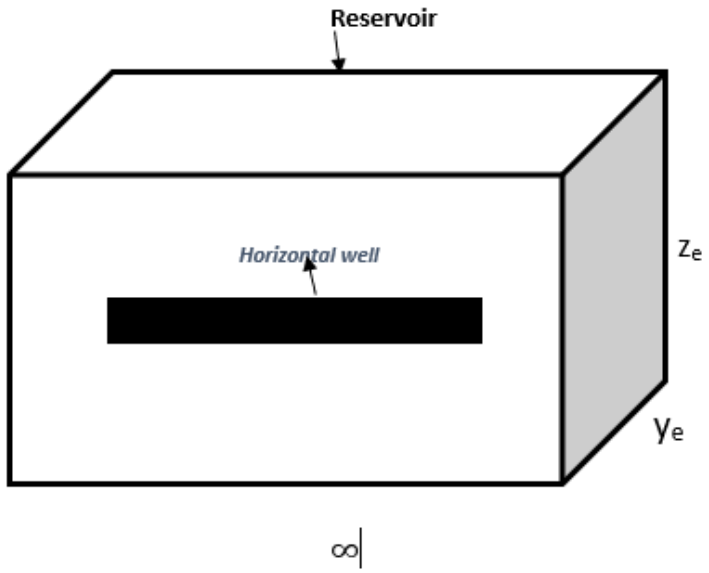

Figure 2:: 3D Reservoir physical model at Early Radial flow along the x-boundary, while y and z-boundaries are sealed

$$S(x_D,\tau_D)=\tfrac{1}{2}[erf(\tfrac{\sqrt{\frac{K}{K_x}}+(x_D-x_{wD})}{2\sqrt{\tau_D}})+erf(\tfrac{\sqrt{\frac{K}{K_x}}+(x_D-x_{wD})}{2\sqrt{\tau_D}})] \qquad (9)$$

Equation (9) is the approximate form for instantaneous source function during early time in the x-boundary.

$$S(y_D,\tau_D)=\tfrac{1}{y_{eD}}[1+2\textstyle\sum_{m=1}^{\infty}\exp(-\frac{m^2\pi^2\tau_D}{y_{eD}^2})\times\cos\frac{m\pi y_{wD}}{y_{eD}}\cos\frac{m\pi y_D}{y_{eD}}] \quad (10)$$

Equation (10) is the infinite plane source in an infinite slab reservoir with y-boundary sealed. The y-boundary has an effect on the flow, therefore the pressure response approximation along the y-boundary is a late-time.

$$S(z_D,\tau_D)=\tfrac{1}{h_D}[1+2\textstyle\sum_{l=1}^{\infty}\exp(-\frac{l^2\pi z_{wD}}{h_D^2})\cos\frac{l\pi z_{wD}}{h_D}\cos\frac{l\pi z_D}{h_D}] \qquad (11)$$

Equation (11) is the infinite plane source in an infinite slab reservoir with z-boundary sealed. The z-boundary has an effect on the flow, therefore the pressure response approximation along the z-boundary is a late-time.

Now by substituting equation (9), (10) and (11) into equation (2), we get.

$$P_D = 2\pi h_D \int_0^{\tau_D} \{ \tfrac{1}{2}[erf(\tfrac{\sqrt{\frac{K}{K_x}}+(x_D-x_{wD})}{2\sqrt{\tau_D}}) + erf(\tfrac{\sqrt{\frac{K}{K_x}}+(x_D-x_{wD})}{2\sqrt{\tau_D}})]\}$$
$$\times \{ \tfrac{1}{y_{eD}}[1 + 2\sum_{m=1}^{\infty} \exp(-\tfrac{m^2\pi^2\tau_D}{y_{eD}^2}) \times \cos\tfrac{m\pi y_{wD}}{y_{eD}} \cos\tfrac{m\pi y_D}{y_{eD}}]\} \times$$
$$\{ \tfrac{1}{h_D}[1 + 2\sum_{l=1}^{\infty} \exp(-\tfrac{l^2\pi z_{wD}}{h_D^2}) \cos\tfrac{l\pi z_{wD}}{h_D} \cos\tfrac{l\pi z_D}{h_D}]\} d\tau_D \quad (12)$$

The first part of equation (12) is the approximate form of instantaneous source function during early-time in the x-boundary, the second part of equation is the late-time approximation of pressure response along the y-boundary and the third is the late-time approximation of pressure response along the z-boundary.

$$P_D' = 2\pi h_D \{ \tfrac{1}{2}[erf(\tfrac{\sqrt{\frac{K}{K_x}}+(x_D-x_{wD})}{2\sqrt{t_D}}) + erf(\tfrac{\sqrt{\frac{K}{K_x}}+(x_D-x_{wD})}{2\sqrt{t_D}})]\}$$
$$\times \{ \tfrac{1}{y_{eD}}[1 + 2\sum_{m=1}^{\infty} \exp(-\tfrac{m^2\pi^2 t_D}{y_{eD}^2}) \times \cos\tfrac{m\pi y_{wD}}{y_{eD}} \cos\tfrac{m\pi y_D}{y_{eD}}]\} \times$$
$$\{ \tfrac{1}{h_D}[1 + 2\sum_{l=1}^{\infty} \exp(-\tfrac{l^2\pi z_{wD}}{h_D^2}) \cos\tfrac{l\pi z_{wD}}{h_D} \cos\tfrac{l\pi z_D}{h_D}]\} \quad (13)$$

The mathematical model defined by equation (12) and (13) will apply in approximating pressure response when y and z-boundaries have and effect on the flow, but x-boundary does not. The flow on the x-boundary is an early time flow regime, but the flow along the y and z-boundaries have a late time flow regime .

Considering a case where y-boundary is not been affected by the flow, but x and z-boundaries are sealed.

$$S(x_{D,\tau_D}) = \tfrac{1}{x_{eD}}[1 + \tfrac{4x_{eD}}{\pi}\sum_{n=1}^{\infty} \exp(-\tfrac{n^2\pi^2\tau_D}{x_{eD}^2}) \sin\tfrac{n\pi}{2x_{eD}} \cos\tfrac{n\pi x_{wD}}{x_{eD}} \cos\tfrac{n\pi x_D}{x_{eD}}] \quad (14)$$

Equation (14) is an infinite plane source in an infinite slab reservoir with x-boundary sealed. Therefore x-boundary has an effect on the flow and the pressure approximation along the x-boundary is a late-time.

$$S(y_D, t_D) = \tfrac{1}{2\sqrt{\pi t_D}}\sqrt{\tfrac{K}{K_y}} e^{-\frac{(y_D-y_{wD})^2}{4_{tD}}} \quad (15)$$

Equation (15) is the approximate form for instantaneous source function during early-time in the y-boundary.

$$S(z_D, t_D) = \tfrac{1}{h_D}[1 + 2\sum_{l=1}^{\infty} \exp(-\tfrac{l^2\pi z_{wD}}{h_D^2}) \cos\tfrac{l\pi z_{wD}}{h_D} \cos\tfrac{l\pi z_D}{h_D}] \quad (16)$$

Equation (16) is an infinite plane source in an infinite slab reservoir with z-boundary sealed. Therefore z-boundary has an effect on the flow and the pressure

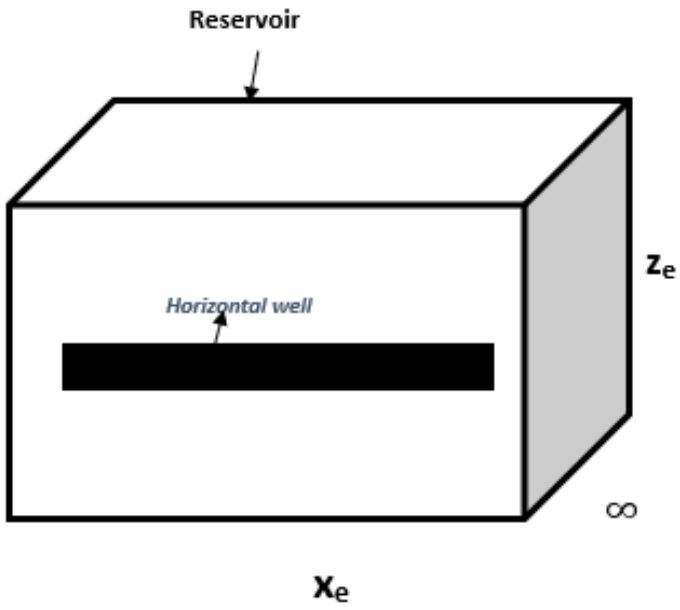

Figure 3:: 3D Reservoir physical model at Infinite-Acting flow along the y-boundary, while x and z-boundaries are sealed

response approximation along the z-boundary is a late-time.

Now by substituting equation (14), (15) and (16) into equation (2), we get.

$$P_D = 2\pi h_D \int_0^{\tau_D} \{ \tfrac{1}{x_{eD}}[1 + \tfrac{4x_{eD}}{\pi} \sum_{n=1}^{\infty} \exp(-\tfrac{n^2\pi^2\tau_D}{x_{eD}^2}) \sin\tfrac{n\pi}{2x_{eD}} \cos\tfrac{n\pi x_{wD}}{x_{eD}} \cos\tfrac{n\pi x_D}{x_{eD}}]\}$$
$$\times \{ \tfrac{1}{2\sqrt{\pi t_D}} \sqrt{\tfrac{K}{K_y}} e^{-\frac{(y_D - y_{wD})^2}{4t_D}}]\}$$
$$\times \{ \tfrac{1}{h_D}[1 + 2\sum_{l=1}^{\infty} \exp(-\tfrac{l^2\pi z_{wD}}{h_D^2}) \cos\tfrac{l\pi z_{wD}}{h_D} \cos\tfrac{l\pi z_D}{h_D}]\} d\tau_D \quad (17)$$

The first part of equation (17) is a case where x-boundary has been sealed and the pressure response approximation is a late-time, the second part is a case where y-boundary has no effect on the flow and the pressure response approximation is an early-time and the third part is a case where z-boundary has been sealed and the pressure response approximation is a late-time.

$$P_D' = 2\pi h_D \{ \tfrac{1}{x_{eD}}[1 + \tfrac{4x_{eD}}{\pi} \sum_{n=1}^{\infty} \exp(-\tfrac{n^2\pi^2 t_D}{x_{eD}^2}) \sin\tfrac{n\pi}{2x_{eD}} \cos\tfrac{n\pi x_{wD}}{x_{eD}} \cos\tfrac{n\pi x_D}{x_{eD}}]\}$$
$$\times \{ \tfrac{1}{2\sqrt{\pi t_D}} \sqrt{\tfrac{K}{K_y}} e^{-\frac{(y_D - y_{wD})^2}{4t_D}}]\}$$
$$\times \{ \tfrac{1}{h_D}[1 + 2\sum_{l=1}^{\infty} \exp(-\tfrac{l^2\pi z_{wD}}{h_D^2}) \cos\tfrac{l\pi z_{wD}}{h_D} \cos\tfrac{l\pi z_D}{h_D}] \quad (18)$$

The mathematical model defined by equation (17) and (18) will apply in approxi-

mating pressure response when x and z-boundaries have an effect on the flow, but y-boundary does not. The flow on the y-boundary is an early time flow regime, but the flow along the x and z-boundaries have a late time flow regime.

Considering a case where z-boundary is not been affected by the flow, but x and y boundaries are sealed.

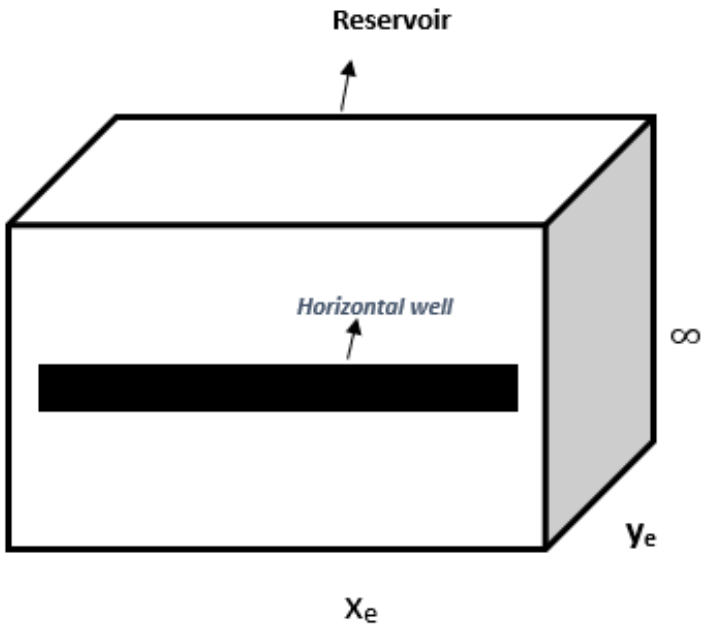

Figure 4:: 3D Reservoir physical model for Infinite-Acting flow along the z-boundary, while x and y-boundaries are sealed

$$S(x_{D,\tau_D}) = \frac{1}{x_{eD}}[1 + \frac{4x_{eD}}{\pi}\sum_{n=1}^{\infty}\exp(-\frac{n^2\pi^2\tau_D}{x_{eD}^2})\sin\frac{n\pi}{2x_{eD}}\cos\frac{n\pi x_{wD}}{x_{eD}}\cos\frac{n\pi x_D}{x_{eD}}] \qquad (19)$$

Equation (19) is the infinite plane source in an infinite slab reservoir with x-boundary sealed. The x-boundary has been affected by the flow, therefore the pressure response approximation along the x-boundary is a late-time.

$$S(y_D, \tau_D) = \frac{1}{y_{eD}}[1 + 2\sum_{m=1}^{\infty}\exp(-\frac{m^2\pi^2\tau_D}{y_{eD}^2}) \times \cos\frac{m\pi y_{wD}}{y_{eD}}\cos\frac{m\pi y_D}{y_{eD}}] \qquad (20)$$

Equation (20) is the infinite plane source in an infinite slab reservoir with y-boundary sealed. The y-boundary has an effect on the flow, therefore the pressure

response approximation along the y-boundary is a late-time.

$$S(z_D, \tau_D) = \frac{1}{2\sqrt{\pi\tau_D}}\sqrt{\frac{K}{K_z}}[\exp(-\frac{(z_D - z_{wD})^2}{4\tau_D})] \tag{21}$$

Equation(21) is the approximate source for instantaneous source function during early-time in z-boundary.

Now by substituting equation (19), (20) and (21) into equation (2), we get.

$$P_D = 2\pi h_D \int_0^{\tau_D} \{ \frac{1}{x_{eD}}[1 + \frac{4x_{eD}}{\pi}\sum_{n=1}^{\infty}\exp(-\frac{n^2\pi^2\tau_D}{x_{eD}^2})\sin\frac{n\pi}{2x_{eD}}\cos\frac{n\pi x_{wD}}{x_{eD}}\cos\frac{n\pi x_D}{x_{eD}}]\}$$
$$\times \{ \frac{1}{y_{eD}}[1 + 2\sum_{m=1}^{\infty}\exp(-\frac{m^2\pi^2\tau_D}{y_{eD}^2}) \times \cos\frac{m\pi y_{wD}}{y_{eD}}\cos\frac{m\pi y_D}{y_{eD}}]\}$$
$$\times \{ \frac{1}{2\sqrt{\pi\tau_D}}\sqrt{\frac{K}{K_z}}[\exp(-\frac{(z_D - z_{wD})^2}{4\tau_D})]\} d\tau_D \tag{22}$$

The first part of equation (22) is a case where the x-boundary has an effect on the flow and the pressure response approximation is a late-time, the second part is a case where the y-boundary has an effect on the flow and the pressure response approximation is a late-time, and the third part is a case where z-boundary has no effect on the flow therefore the pressure approximation will be an early-time.

$$P_D' = 2\pi h_D \{ \frac{1}{x_{eD}}[1 + \frac{4x_{eD}}{\pi}\sum_{n=1}^{\infty}\exp(-\frac{n^2\pi^2 t_D}{x_{eD}^2})\sin\frac{n\pi}{2x_{eD}}\cos\frac{n\pi x_{wD}}{x_{eD}}\cos\frac{n\pi x_D}{x_{eD}}]\}$$
$$\times \{ \frac{1}{y_{eD}}[1 + 2\sum_{m=1}^{\infty}\exp(-\frac{m^2\pi^2 t_D}{y_{eD}^2}) \times \cos\frac{m\pi y_{wD}}{y_{eD}}\cos\frac{m\pi y_D}{y_{eD}}]\}$$
$$\times \{ \frac{1}{2\sqrt{\pi t_D}}\sqrt{\frac{K}{K_z}}[\exp(-\frac{(z_D - z_{wD})^2}{4t_D})]\} \tag{23}$$

The mathematical model defined by equation (22) and (23) will apply in approximating pressure response when x and y-boundaries have an effect on the flow, but z-boundary does not. The flow on the z-boundary is an early time flow regime, while the flow on the x and y-boundaries are late time flow regime.

Late Time Approximation for Pressure

Considering a case where both x,y and z-boundaries are sealed.

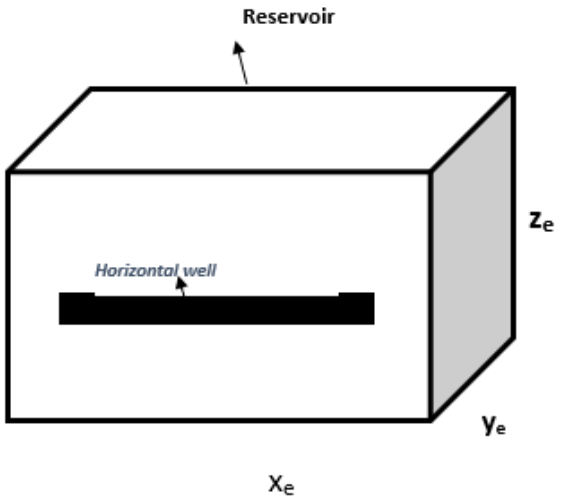

Figure 5:: 3D Reservoir physical model for Steady-state flow

$$S(x_{D,\tau_D}) = \frac{1}{x_{eD}}[1 + \frac{4x_{eD}}{\pi}\sum_{n=1}^{\infty}\exp(-\frac{n^2\pi^2\tau_D}{x_{eD}^2})\sin\frac{n\pi}{2x_{eD}}\cos\frac{n\pi x_{wD}}{x_{eD}}\cos\frac{n\pi x_D}{x_{eD}}]d\tau_D \quad (24)$$

Equation (24) is an infinite plane source in an infinite slab reservoir with x-boundary sealed. The x-boundary has an effect on the flow therefore the pressure response approximation is a late-time.

$$S(y_D, \tau_D) = \frac{1}{y_{eD}}[1 + 2\sum_{m=1}^{\infty}\exp(-\frac{m^2\pi^2\tau_D}{y_{eD}^2}) \times \cos\frac{m\pi y_{wD}}{y_{eD}}\cos\frac{m\pi y_D}{y_{eD}}]d\tau_D \quad (25)$$

Equation (25) is an infinite plane source in an infinite slab reservoir with y-boundary sealed. Then y-boundary has an effect on the flow therefore the pressure response approximation is a late-time.

$$S(z_D, \tau_D) = \frac{1}{h_D}[1 + 2\sum_{l=1}^{\infty}\exp(-\frac{l^2\pi z_{wD}}{h_D^2})\cos\frac{l\pi z_{wD}}{h_D}\cos\frac{l\pi z_D}{h_D}]d\tau_D \quad (26)$$

Equation (26) is an infinite plane source in an infinite slab reservoir with z-boundary sealed. Then z-boundary has an effect on the flow therefore the pressure response approximation is a late-time.

Now by substituting equation (24), (25) and (26) into equation (2), we get.

$$P_D = 2\pi h_D \int_0^{\tau_D} \{ \frac{1}{x_{eD}}[1 + \frac{4x_{eD}}{\pi}\sum_{n=1}^{\infty}\exp(-\frac{n^2\pi^2\tau_D}{x_{eD}^2})\sin\frac{n\pi}{2x_{eD}}\cos\frac{n\pi x_{wD}}{x_{eD}}\cos\frac{n\pi x_D}{x_{eD}}]\}$$
$$\times \{ \frac{1}{y_{eD}}[1 + 2\sum_{m=1}^{\infty}\exp(-\frac{m^2\pi^2\tau_D}{y_{eD}^2}) \times \cos\frac{m\pi y_{wD}}{y_{eD}}\cos\frac{m\pi y_D}{y_{eD}}]\}$$
$$\times \{ \frac{1}{h_D}[1 + 2\sum_{l=1}^{\infty}\exp(-\frac{l^2\pi z_{wD}}{h_D^2})\cos\frac{l\pi z_{wD}}{h_D}\cos\frac{l\pi z_D}{h_D}]\}d\tau_D \quad (27)$$

Equation (27) is an infinite plane source in an infinite slab reservoir with all the boundaries sealed. All the boundaries has an effect on the flow, therefore the pressure response approximation on all the boundaries is a late-time, it is the case where the reservoir has attained the pseudo steady-state flow.

$$P'_D = 2\pi h_D\{\ \tfrac{1}{x_{eD}}[1+\tfrac{4x_{eD}}{\pi}\sum_{n=1}^{\infty}\exp(-\tfrac{n^2\pi^2 t_D}{x_{eD}^2})\sin\tfrac{n\pi}{2x_{eD}}\cos\tfrac{n\pi x_{wD}}{x_{eD}}\cos\tfrac{n\pi x_D}{x_{eD}}]\}$$
$$\times\{\ \tfrac{1}{y_{eD}}[1+2\sum_{m=1}^{\infty}\exp(-\tfrac{m^2\pi^2 t_D}{y_{eD}^2})\times\cos\tfrac{m\pi y_{wD}}{y_{eD}}\cos\tfrac{m\pi y_D}{y_{eD}}]\}$$
$$\times\{\ \tfrac{1}{h_D}[1+2\sum_{l=1}^{\infty}\exp(-\tfrac{l^2\pi z_{wD}}{h_D^2})\cos\tfrac{l\pi z_{wD}}{h_D}\cos\tfrac{l\pi z_D}{h_D}]\} \quad (28)$$

The mathematical model defined by equation (27) and (28) will apply in approximating pressure response when x, y and z-boundaries both have an effect on the flow. The flow on both of the boundaries are late time flow regime. Equation (27) and (28) is the pressure distribution model for completely bounded reservoir where there is a constant pressure at each and every point of the reservoir.

Dimensionless Parameters

$$P_D = \frac{kh\Delta p}{141.2q\mu B} \quad (29)$$

$$t_D = \frac{4kt_i}{\phi\mu c_t L^2} \quad (30)$$

$$\eta_i = \frac{k_i}{\phi\mu c_t} \quad (31)$$

$$i_D = \frac{2i}{L}\sqrt{\frac{k}{k_i}} \quad (32)$$

$$i_{wD} = \frac{2i_w}{L}\sqrt{\frac{k}{k_i}} \quad (33)$$

$$i_{eD} = \frac{2i_e}{L}\sqrt{\frac{k}{k_i}} \quad (34)$$

$$h_D = \frac{2h}{L}\sqrt{\frac{k}{k_z}} \quad (35)$$

$$L_D = \frac{L}{2h}\sqrt{\frac{k}{k_x}} \quad (36)$$

$$h_D = \frac{1}{L_D}\sqrt{\frac{k^2}{k_x k_z}} \quad (37)$$

$$r_{wD} = z_D - z_{wD} \quad (38)$$

$$\eta = \frac{k_i}{\mu\phi c_t} \quad (39)$$

IV. RESULTS AND DISCUSSIONS

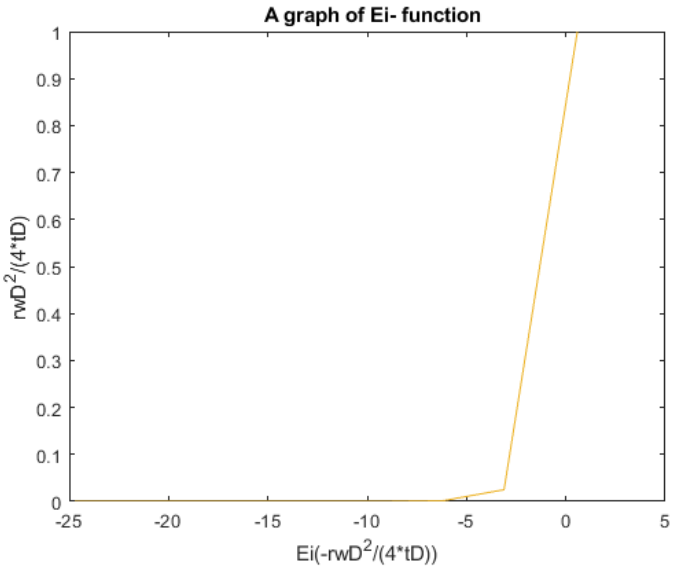

Figure 6:: A graph of Ei-function

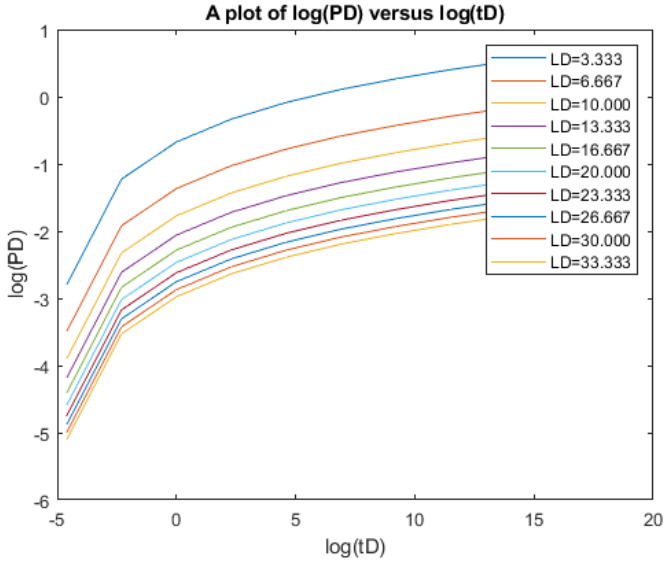

Figure 7:: Dimensionless pressure grows with dimensionless time

Early Time Radial Flow

The flow is radial in the $y-z$ plane and can be considered as the early radial flow period. Considering the equation for dimensionless pressure during infinite-acting flow period, and using the approximation of the exponential integral for $\frac{r_{wD}^2}{4t_D} > 0.02$, the exponential integral can be approximated as.

$$Ei(-\frac{r_{wD}^2}{4t_D}) = ln(\frac{r_{wD}^2}{4t_D}) + 0.577$$

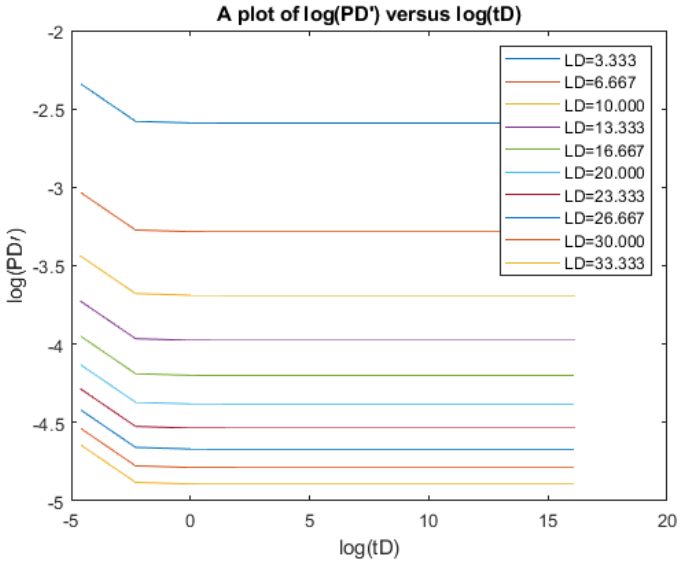

Figure 8:: $P_D^{'}$ is a constant with an increased t_D

$$P_D = \frac{1}{4L_D}[-Ei(-\frac{r_{wD}^2}{4t_D})]$$

$$P_D^{'} = \frac{1}{4L_D}exp[-\frac{r_{wD}^2}{4t_D}]$$

The Ei-function solution is presented in figure 6, it shows that $\frac{r_{wD}^2}{4t_D}$ is directly proportional to $Ei(-\frac{r_{wD}^2}{4t_D})$. Figure 7 represents the growth of dimensionless pressure with an increase in dimensionless time on the log-log plots. From figure 7, we noticed that L_D increased from 3.333 to 33.333, we also observed that $log(P_D)$ is directly proportional to $log(t_D)$. Figure 8 represents the constant $P_D^{'}$ with an increased in t_D, also in figure 8 $log(P_D^{'})$ decreased within a very short period of time and then becomes a constant with an increased t_D.

We consider theoretical well and reservoir parameters and substitute them in the models formulated in the previous chapter, and compute the dimensionless pressure and its derivative. By using log-log plots we analyze the effects of the well and reservoir parameters on the well performance. We solved the dimensionless parameters by taking the reservoir permeability $K = \sqrt{k_y k_z}$, $k_x = k_y = k_z = 20md$, height $h = 75ft$, reservoir length $x_e = 5000ft$, reservoir width $y_e = 3500ft$, and reservoir thickness $z_e = 2000ft$. We take the length of the well from 500 to $5000ft$

Dimensionless parameters for varying L_D

$k = \sqrt{k_y k_z}$, $k_x = k_y = k_z = 20md$, $h = 75ft$, $x_e = 5000ft$, $y_e = 3500ft$,

$z_e = 2000$, $z_w = 400ft$ and z=450md

Table 1:: Dimensionless parameters for varying L_D

$L(ft)$	500	1000	1500	2000	2500	3000	3500	4000	4500	5000
L_D	3.333	6.667	10.000	13.333	16.667	20.000	23.333	26.667	30.000	33.333
h_D	0.300	0.150	0.100	0.075	0.060	0.050	0.043	0.038	0.033	0.030
x_D	0.5	0.5	0.5	0.5	0.5	0.5	0.5	0.5	0.5	0.5
y_D	7.000	3.500	2.334	1.750	1.400	1.167	1.000	0.875	0.778	0.700
z_D	1.800	0.900	0.600	0.450	0.360	0.300	0.257	0.225	0.200	0.180
x_{wD}	0.5	0.5	0.5	0.5	0.5	0.5	0.5	0.5	0.5	0.5
y_{wD}	7.000	3.500	2.334	1.750	1.400	1.167	1.000	0.875	0.778	0.700
z_{wD}	1.600	0.800	0.533	0.400	0.320	0.267	0.229	0.200	0.178	0.160
x_{eD}	20.000	10.000	6.667	5.000	4.000	3.333	2.857	2.500	2.222	2.000
y_{eD}	14.000	7.000	4.667	3.500	2.800	2.333	2.000	1.750	1.556	1.400
z_{eD}	8.000	4.000	2.667	2.000	1.600	1.333	1.143	1.000	0.889	0.800
r_{wD}	0.200	0.100	0.067	0.050	0.040	0.033	0.028	0.025	0.022	0.020
α_1	0.0004	0.003	0.010	0.021	0.038	0.058	0.079	0.100	0.116	0.125
α_2	11.112	44.447	100.01	177.799	277.816	400.058	540.912	692.621	918.390	1111.236

t_D	P_D	$P_D^{'}$
1.0×10^{-2}	0.060703	0.096312
1.0×10^{-1}	0.293492	0.075854
1.0×10^{00}	0.510108	0.075054
1.0×10^{01}	0.716294	0.075011
1.0×10^{02}	0.917864	0.075008
1.0×10^{03}	1.115223	0.075008
1.0×10^{04}	1.304935	0.075008
1.0×10^{05}	1.496823	0.075008
1.0×10^{06}	1.683832	0.075008
1.0×10^{07}	1.872349	0.075008

(a) Table 2:The values of P_D and $P_D^{'}$ when $L_D = 3.3330$

t_D	P_D	$P_D^{'}$
1.0×10^{-2}	0.030347	0.048149
1.0×10^{-1}	0.146724	0.037921
1.0×10^{00}	0.255016	0.037522
1.0×10^{01}	0.358093	0.037500
1.0×10^{02}	0.458863	0.037498
1.0×10^{03}	0.557528	0.037498
1.0×10^{04}	0.652370	0.037498
1.0×10^{05}	0.748299	0.037498
1.0×10^{06}	0.841790	0.037498
1.0×10^{07}	0.936034	0.037498

(b) Table 3: The values of P_D and $P_D^{'}$ when $L_D = 6.6670$

t_D	P_D	$P_D^{'}$
1.0×10^{-02}	0.020232	0.032101
1.0×10^{-01}	0.097821	0.025282
1.0×10^{00}	0.170019	0.025016
1.0×10^{01}	0.238741	0.025001
1.0×10^{02}	0.305924	0.025000
1.0×10^{03}	0.371704	0.025000
1.0×10^{04}	0.434935	0.025000
1.0×10^{05}	0.498891	0.025000
1.0×10^{06}	0.561221	0.025000
1.0×10^{07}	0.624054	0.025000

(a) Table 4: The values of P_D and $P_D^{'}$ when $L_D = 10.0000$

t_D	P_D	$P_D^{'}$
1.0×10^{-02}	0.015175	0.024076
1.0×10^{-01}	0.073367	0.018962
1.0×10^{00}	0.127517	0.018762
1.0×10^{01}	0.179060	0.018751
1.0×10^{02}	0.229449	0.018751
1.0×10^{03}	0.278785	0.018750
1.0×10^{04}	0.326209	0.018750
1.0×10^{05}	0.374178	0.018750
1.0×10^{06}	0.420926	0.018750
1.0×10^{07}	0.468052	0.018750

(b) Table 5: The values of P_D and $P_D^{'}$ when $L_D = 13.3330$

t_D	P_D	$P_D^{'}$
1.0×10^{-02}	0.012139	0.019260
1.0×10^{-01}	0.058691	0.015169
1.0×10^{00}	0.102009	0.015009
1.0×10^{01}	0.143242	0.015000
1.0×10^{02}	0.183551	0.015000
1.0×10^{03}	0.223018	0.015000
1.0×10^{04}	0.260956	0.015000
1.0×10^{05}	0.299329	0.015000
1.0×10^{06}	0.336726	0.015000
1.0×10^{07}	0.374425	0.015000

(a) Table 6: The values of P_D and $P_D^{'}$ when $L_D = 16.6670$

t_D	P_D	$P_D^{'}$
1.0×10^{-02}	0.010116	0.016050
1.0×10^{-01}	0.048910	0.012641
1.0×10^{00}	0.085009	0.012508
1.0×10^{01}	0.119370	0.012501
1.0×10^{02}	0.152962	0.012500
1.0×10^{03}	0.185852	0.012500
1.0×10^{04}	0.217467	0.012500
1.0×10^{05}	0.249446	0.012500
1.0×10^{06}	0.280611	0.012500
1.0×10^{07}	0.312027	0.012500

(b) Table 7: The values of P_D and $P_D^{'}$ when $L_D = 20.0000$

t_D	P_D	$P_D^{'}$
1.0×10^{-02}	0.008671	0.013758
1.0×10^{-01}	0.041924	0.010835
1.0×10^{00}	0.072866	0.010721
1.0×10^{01}	0.102319	0.010715
1.0×10^{02}	0.131112	0.010714
1.0×10^{03}	0.159304	0.010714
1.0×10^{04}	0.186403	0.010714
1.0×10^{05}	0.213814	0.010714
1.0×10^{06}	0.240527	0.010714
1.0×10^{07}	0.267456	0.010714

(a) Table 8: The values of P_D and $P_D^{'}$ when $L_D = 23.3330$

t_D	P_D	$P_D^{'}$
1.0×10^{-02}	0.007587	0.012038
1.0×10^{-01}	0.036682	0.009481
1.0×10^{00}	0.063756	0.009381
1.0×10^{01}	0.089527	0.009375
1.0×10^{02}	0.114720	0.009375
1.0×10^{03}	0.139387	0.009375
1.0×10^{04}	0.163099	0.009375
1.0×10^{05}	0.187082	0.009375
1.0×10^{06}	0.210455	0.009375
1.0×10^{07}	0.234017	0.009375

(b) Table 9: The values of P_D and $P_D^{'}$ when $L_D = 26.6670$

t_D	P_D	$P_D^{'}$
1.0×10^{-02}	0.006744	0.010700
1.0×10^{-01}	0.032607	0.008427
1.0×10^{00}	0.056673	0.008339
1.0×10^{01}	0.079580	0.008334
1.0×10^{02}	0.101975	0.008333
1.0×10^{03}	0.123901	0.008333
1.0×10^{04}	0.144978	0.008333
1.0×10^{05}	0.166297	0.008333
1.0×10^{06}	0.187074	0.008333
1.0×10^{07}	0.208018	0.008333

(a) Table 10: The values of P_D and $P_D^{'}$ when $L_D = 30.0000$

t_D	P_D	$P_D^{'}$
1.0×10^{-02}	0.006070	0.009630
1.0×10^{-01}	0.029347	0.007585
1.0×10^{00}	0.051006	0.007505
1.0×10^{01}	0.071623	0.007500
1.0×10^{02}	0.091778	0.007500
1.0×10^{03}	0.111512	0.007500
1.0×10^{04}	0.130482	0.007500
1.0×10^{05}	0.149669	0.007500
1.0×10^{06}	0.168368	0.007500
1.0×10^{07}	0.187218	0.007500

(b) Table 11: The values of P_D and $P_D^{'}$ when $L_D = 33.3330$

We observed that from Table 2 to Table 11, as L_D increases both P_D and $P_D^{'}$ decreases during the infinite-acting flow period. Dimensionless horizontal well length is inversely proportional to both the Dimensionless pressure and Dimensionless pressure derivatives. During early radial flow period dimensionless pressure grows with dimensionless time, whiles dimensionless pressure derivatives stabilizes and kept constant during early radial flow period, this is the time when the well is initially open for production and non of the reservoir boundaries is been affected by the flow. Therefore early radial flow period has a slope of zero.

V. CONCLUSION

We studied early radial flow period by both analytical and numerical methods. We use Source and Green's function with Newmann's product to analytically formulate the early radial flow model. The parameters of the early radial flow were implemented on matlab. We solved well test analysis of a horizontal well in a completely bounded isotropic reservoir by both analytical and numerical methods, and the numerical results shows that as we increased L_D both P_D and P_D' decreases. We compare our solution with several other numerical approaches that had been used in the past to solve well test analysis of a horizontal well in a completely bounded isotropic reservoir like Gauss-Legendre quadrature, Laplace transform and finite difference methods.

REFERENCES

[1] Aghar,H.,Carie,M.,Elshahawi,H.,Gomez,J.R.,Saeedi,J.,Young,C.,...Theuveny,B. The expanding scope of well testing. In oilfield review (Vol.19,pp.44-59),(2007)

[2] Akin,S. Design and analysis of multi-well interference tests. In proceedings of the world geothermal congress,melbourne,autralia(pp.19-25), (2015)

[3] Bourdet,D. Well test analysis: the use of advanced interpretation models, Elsevier,(2002)

[4] Cheng,Y. Pressure transient testing and productivity analysis for horizontal wells. Texas A and M university,(2003)

[5] Duan,Y.G.,Ren,K.Y.,Fang,Q.T.,Wei,M.Q.,Dejam,M.,Chen,W.H. Pressure transient analysis for a horizontal well in heterogenous carbonate reservoir using a linear composite model. Mathematical problems in engineering,(2020)

[6] Eiroboyi,I., Obeta,P. The performance of a vertical well subject to edge water drive. In Advanced materials research (Vol.1025,pp.974-978),(2014)

[7] Gao,Y.,Rahman,M.M.,Lu,J. Novel mathematical model for transient pressure analysis of multifractured horizontal wells in naturally fractured oil reservoirs. ACS Omega,6(23),15205-15221,(2021)

[8] Gilman,J.R.,Jargon,J.R. Evaluating horizontal versus vertical well performance. World Oil,213(6):55-60,(1992)

[9] Idudje,E.,Adewole,E. A new test analysis procedure for pressure drawdown test of a horizontal well in an infinite-acting reservoir, Nigerian Journal of Technology,39(3),816-820,(2020)

[10] Igba,S.,Akanji,L.,Onwuliri,T. Horizontal versus vertical wells interference in hydraulically fractured shale reservoirs, Journal of Oil, Gas and Petrochemical

Sciences,(2019)

[11] Kutasov,I.,Eppelbaum,L.,Kagan,M.Interference well testing-variable fluid flow rate, Journal of Geophysics and Engineering,5(1),86-91,(2008)

[12] Lee,W.J. Well testing. Society of Petroleum Engineering of AIME, New York,(1982)

[13] Li,X.P.,Yan,N.P.,Tan,X.H. Characteristic value method of well test analysis for horizontal gas well. Mathematical problems in engineering,(2014)

[14] Mach,J.,Promo,E.,Brown,K.E. A nodal approach for applying systems analysis to the flowing and artificial lift oil or gas well. Society of petroleum engineers,(1979)

[15] Mohammed,I.,Olayiwola,T.O,Alkathim,M.,Awotunde,A.A.,Alafnan,S.F. A review of pressure transient analysis in reservoirs with natural fractures,vugs and/or caves. Petroleum Science,18(1),154-172,(2021)

[16] Nzomo,T.K.,Adewole,S.E.,Awuor,K.O.,Oyoo,D.O. Performance of a horizontal well in a bounded anisotropic reservoir:part i: Mathematical analysis. Open Engineering,12(1),17-28,(2022)

[17] Nie,R,S.,Guo,J.C.,Jia,Y.L.,Zhu,S.Q.,Rao,Z.,Zhang,C.G. New modelling of transient well test and rate decline analysis for a horizontal well in a multiple-zone reservoir. Journal of Geophysics and Engineering,8(3),464,(2011)

[18] Ogbamikhumi,A.,Adewole,E. Pressure bahaviour of a horizontal well sandwiched between two parallel sealing faults. Nigerian Journal of Technology,39(1),148-153,(2020)

[19] Orene,J.,Adewole,E. Pressure distribution of a horizontal well in a bounded reservoir with constant pressure top and bottom. Nigerian Journal of Technology,39(1),154-

160,(2020)

[20] Ouyang,W.,Sun,H.,Han,H. A new well test interpretation model for complex fracture networks in horizontal wells with multi-stage volume fracturing in tight gas reservoirs. Natural gas Industry B, 7(5),514-522,(2020)

[21] Sanni,M.O.,Gringarten,A.C. Well test analysis in volatile oil reservoirs. In Spe annual technical conference and exhibition,(2008)

[22] Soleiman,R.,Jahanpeyma,Y.,Salehian,M. Analysis of horizontal well productivity in tight gas formations and its sensitivity to reservoir properties. Journal of petroleum exploration and production technology,9(2),1237-1244,(2019)

[23] Temizel,C.,Irani,M.,Ghannadi,S.,Canbaz,C.H.,Moreno,R.,Bashtani,F.,Basri,M.A. Optimization of steam-additive processes with dts/das applications in heavy oil reservoirs. In Spe annual technical conference and exhibition,(2019)

[24] Zhang,J.,Cheng,S.,Di,S.,Gao,Z.,Yang,R.,Cao,P. A two-phase numerical model of well test analysis to characterize formation damage in near well regions of injection wells. Geofluids,(2021)

[25] Zhuo,L.,Yu,J.,Zhang,H.,Zhou,C. Influence of horizontal well section length on the depressurization development effect on natural gas hydrate reservoirs. Natural Gas Industry b, 8(5), 505-513,(2021)